# Radio Channel Emulation for Virtual Drive Testing with Site-Specific Channels

Mbugua, Allan Wainaina; Chen, Yun; Fan, Wei

*Published in:*
16th European Conference on Antenna and Propagation

*DOI (link to publication from Publisher):*
10.23919/EuCAP53622.2022.9769382

*Publication date:*
2022

*Document Version*
Accepted author manuscript, peer reviewed version

# Radio Channel Emulation for Virtual Drive Testing with Site-Specific Channels

Allan Wainaina Mbugua*†, Yun Chen*, Wei Fan†,
*Huawei Technologies Duesseldorf GmbH, Munich Research Center, Munich, Germany, allan.mbugua@huawei.com
†Antennas Propagation and Millimetre-Wave Section, Aalborg University, Aalborg, Denmark, wfa@es.aau.dk

***Abstract*—Virtual drive testing (VDT) with measured or ray tracing (RT) simulated channels requires the simplification of the channel to match the hardware specification of radio channel emulators. That is, reduction of the number of multipath components (MPC)s and adjustment of the arbitrary delays of the MPCs to the sampling grid of the radio channel emulator. In this paper, a fractional delay (FD) filter approximated by a general least square (GLS) finite impulse response (FIR) filter is used for band-limited interpolation to align the delay of the MPCs to the sampling grid of the radio channel emulator. A dominant power selection strategy is then employed to reduce the taps to match a given hardware specification. The GLS FIR method is shown to have superior performance in preservation of the channel frequency response (CFR) compared to rounding delays to the nearest integer multiple of the sampling time.**

***Index Terms*—Radio channel emulation, radio channel modeling, ray tracing, virtual drive testing.**

## I. Introduction

Radio channel emulation is a key technology in the testing of wireless communication systems due to the ability to generate arbitrary fading conditions in laboratory setups [1]. This enables novel applications such as virtual drive testing (VDT), whereby measured or ray tracing (RT) channels are used in optimization of radio networks [2], [3], [4], [5]. Advances in state-of-the-art RT techniques has led to high fidelity channel prediction [6]. Dynamic RT is further envisioned to facilitate rapid generation of RT channels which can be used in VDT thus reducing costly drive tests in the field [7].

RT simulated channels are characterized by rays with an infinite delay resolution and possibly in the order of hundreds or thousands per transmitter (Tx) and receiver (Rx) antenna pair especially when diffraction and diffuse scattering are enabled [8]. Similarly in measured channels, depending on the delay resolution and dynamic range of the channel sounder, a high number of multipath component (MPC)s may be estimated. Pre-processing prior to emulation is thus necessary to match the output of the RT to the hardware specification of radio channel emulators. In particular the delays of MPCs are arbitrary while in radio channel emulators delays must be in integer multiples of the sampling time [9]. Secondly, the number of MPCs from site specific channels must be reduced to match at most the maximum number supported by a given hardware e.g. 24 or 48 taps [10], [11]. This limit stems from the fact that each tap is implemented using hardware multipliers in field programmable gate arrays (FPGAs) [12]. In [13], the limitation on the number of MPCs that can be implemented on FPGAs based channel emulators is mitigated by a subspace representation of the time-variant channel impulse response (CIR). However, in most commercial file-based channel emulators, the degree of freedom available to users is limited to the delay and the complex coefficients of the CIR.

Delay alignment of MPCs in measured or RT simulated channels can intuitively be carried out by rounding the delays to the nearest sampling instance of a given fading emulator. However, this often results in a distortion of the phase of the channel thus causing differences between the target channel frequency response (CFR) and the realized CFR in the fading emulator. In digital file-based radio channel emulators, fractional delay (FD) filters are a natural choice for performing delay alignment of MPCs which is essentially a band-limited interpolation problem [14]. The FD filter coefficients can be computed offline and stored in a file for real-time replay during radio channel emulation.

The impulse response of the ideal FD is a Sinc function which is non-causal and results in an infinite number of non-zero coefficients when the FD of a given MPC is not zero. That is, the delay of the MPC is not an integer multiple of the sampling time. Several types of finite impulse response (FIR) can be used to approximate the ideal FD filter [14]. In emulation of radio channels preservation of the target CFR is key mainly due to the fact signal processing is done in the frequency domain e.g. in radio technologies employing orthogonal frequency division multiplexing (OFDM). In [15], a FIR is realized by truncation of the ideal FD filter followed by an iterative path reduction and the phase of the surviving paths are convex optimized to match a target CFR. However, FIR design by truncation of the ideal FD delay filter is prone to the Gibb's phenomena [16].

In this paper, a method of delay alignment of site-specific radio channels using a general least squares (GLS) FIR filter and subsequent tap reduction based on the power, is shown to achieve reproduction of the CFR with high fidelity even with a limited number of taps. This is in contrast to the rounding delays to the nearest sampling instance which suffers from significant magnitude errors even with availability of more tap resources. One drawback of the GLS FIR filter based approach is that it requires matrix inversion in determining the tap coefficients which may fail when the matrix is ill-conditioned.

## II. System Model

### A. Channel Model

Consider a multiple-input multipe-output (MIMO) system with $K$ base station (BS) and $L$ mobile terminal (MT) antennas, respectively. Given that the channel is composed of $M$ MPCs, the time variant CFR between the BS antenna $k \in [1, K]$ and MT antenna $l \in [1, L]$ can be obtained as:

$$H_{k,l}(t,f) = \sum_{m=1}^{M} \begin{bmatrix} F_l^{\mathrm{V}}(\mathbf{\Omega}_{\mathrm{Rx}}, f) \\ F_l^{\mathrm{H}}(\mathbf{\Omega}_{\mathrm{Rx}}, f) \end{bmatrix}^T \begin{bmatrix} \alpha_m^{\mathrm{VV}}(t,f) & \alpha_m^{\mathrm{VH}}(t,f) \\ \alpha_m^{\mathrm{HV}}(t,f) & \alpha_m^{\mathrm{HH}}(t,f) \end{bmatrix} \begin{bmatrix} F_k^{\mathrm{V}}(\mathbf{\Omega}_{\mathrm{Tx}}, f) \\ F_k^{\mathrm{H}}(\mathbf{\Omega}_{\mathrm{Tx}}, f) \end{bmatrix} \cdot \exp\left(-j2\pi f \tau_m\right) \cdot \exp\left(-j2\pi v_m t\right) \tag{1}$$

where $f$ is the frequency, $\alpha_m^{\mathrm{VV}}$ and $\alpha_m^{\mathrm{HH}}$ are the vertical and horizontal co-polar components, respectively, while $\alpha_m^{\mathrm{VH}}$ and $\alpha_m^{\mathrm{HV}}$, are the vertical and horizontal cross-polar components, respectively. $\tau_m$, and $v_m$ are the delay and Doppler frequency, respectively, while $F^{\mathrm{V}}$ and $F^{\mathrm{H}}$ are the complex antenna radiation pattern components for the vertical and horizontal polarization, respectively. $\mathbf{\Omega}_{\mathrm{Rx}} = [\theta, \phi]$ and $\mathbf{\Omega}_{\mathrm{Tx}} = [\theta, \phi]$ are the angle of arrival and departure, respectively, where $\theta$ and $\phi$ are the elevation and azimuth angles, respectively. In this paper the time dependence in (1) is assumed to be the time series of $R$ CFR responses that need to be emulated.

### B. Delay Alignment and Tap Selection

The CFR in (1) is not realizable in practical radio channel emulators since the delay of the $M$ MPCs is not guaranteed to be in integer multiples of the sampling time. For an ideal FD filter the CFR due to the $m$-th MPC can be obtained as [14]:

$$\bar{H}_{k,l}^{m}(t,\omega) = \sum_{n=-\infty}^{\infty} h[n] \exp(-j\omega n) \tag{2}$$

where $\omega \in [0, 1]$ is the normalized frequency and $h$ is the filter coefficient for the $n$-th sampling instance. The CFR in (2) of the ideal FD cannot be realized on realistic radio channel emulators as it requires an infinite number of coefficients and would be non-causal.

For a finite and causal filter with even length $N$, the CFR due to the $m$-th MPC can be obtained as [17]:

$$\hat{H}_{k,l}^{m}(t,\omega) = h[0] + 2\sum_{n=1}^{N/2} h[n]\cos(\omega n) \tag{3}$$

where the length $N$ can be obtained from the RT simulated or measured channel as:

$$N = \lceil D_{\max} \rceil \tag{4}$$

with $D_{\max} = \tau_{\max} f_s$ whereby $f_s$ is the channel emulator's sampling frequency. For $P$ frequencies, (3) can be written as:

$$\hat{\mathbf{c}}_{k,l}^{m}(t) = \mathbf{A}\mathbf{h}_{k,l}^{m}(t) \tag{5}$$

where $\mathbf{A} \in \mathbb{R}^{P \times N/2}$ is defined as:

$$\mathbf{A} = \begin{bmatrix} 1 & 2\cos(\omega_0) & \cdots & 2\cos[\omega_0(N/2)] \\ 1 & 2\cos(\omega_1) & \cdots & 2\cos[\omega_1(N/2)] \\ \vdots & \vdots & & \vdots \\ 1 & 2\cos(\omega_{P-1}) & \cdots & 2\cos[\omega_{P-1}(N/2)] \end{bmatrix} \tag{6}$$

with $\hat{\mathbf{c}}_{k,l}^{m}(t)$ and $\mathbf{h}_{k,l}^{m}(t)$ defined as:

$$\hat{\mathbf{c}}_{k,l}^{m}(t) = \begin{bmatrix} \hat{H}_{k,l}^{m}(t,\omega_1) & \hat{H}_{k,l}^{m}(t,\omega_2) & \cdots & \hat{H}_{k,l}^{m}(t,\omega_P) \end{bmatrix}^T \tag{7}$$

and

$$\mathbf{h}_{k,l}^{m}(t) = \begin{bmatrix} h[0] & h[1] & \cdots & h[N/2] \end{bmatrix}^T, \tag{8}$$

respectively. The estimate of the FIR coefficients $\mathbf{h}_{k,l}^{m}(t)$ can be obtained by solving the (5) by the GLS method which yields the optimal solution as:

$$\hat{\mathbf{h}}_{k,l}^{m}(t) = \arg\min_{\mathbf{h}_{k,l}^{m}(t)} \quad ||\mathbf{A}\mathbf{h}_{k,l}^{m}(t) - \hat{\mathbf{c}}_{k,l}^{m}(t)||_2^2 \quad . \tag{9}$$

Note that due to the symmetry of the problem (3), the rest $N/2$ coefficients can be easily obtained. The filter coefficients for each sampling instance due to the $M$ MPCs can be obtained as:

$$\hat{\mathbf{h}}_{k,l}(t) = \sum_{m=1}^{M} \hat{\mathbf{h}}_{k,l}^{m}(t). \tag{10}$$

The equivalent CFR (1) with delay alignment can be reformulated as:

$$H_{k,l}^{Eq}(t,f) = \sum_{n=0}^{N-1} \hat{h}_{k,l}^{n}(t) \exp\left(-j2\pi f \tau_n\right) \sum_{m=1}^{M} \begin{bmatrix} F_l^{\mathrm{V}}(\mathbf{\Omega}_{\mathrm{Rx}}, f) \\ F_l^{\mathrm{H}}(\mathbf{\Omega}_{\mathrm{Rx}}, f) \end{bmatrix}^T \begin{bmatrix} \alpha_m^{\mathrm{VV}}(t,f) & \alpha_m^{\mathrm{VH}}(t,f) \\ \alpha_m^{\mathrm{HV}}(t,f) & \alpha_m^{\mathrm{HH}}(t,f) \end{bmatrix} \begin{bmatrix} F_k^{\mathrm{V}}(\mathbf{\Omega}_{\mathrm{Tx}}, f) \\ F_k^{\mathrm{H}}(\mathbf{\Omega}_{\mathrm{Tx}}, f) \end{bmatrix} \cdot \exp\left(-j2\pi v_m t\right) \tag{11}$$

In state-of-the-art radio channel emulators the number of taps supported $Q$, is often lower than the number of non-zero coefficients which equal to at most $N$ especially in urban macrocell (UMa) scenarios where the filter length can be long. Based on the observation that the MPCs with the highest power have the most significant contribution to the CFR the equivalent CFR (11), can be approximated with $Q \subseteq N$ most dominant taps. The emulated CFR is thus given as:

$$H_{k,l}^{emu}(t,f) = \sum_{q=1}^{Q} \hat{h}_{k,l}^{q}(t) \exp\left(-j2\pi f \tau_q\right) \sum_{m=1}^{M} \begin{bmatrix} F_l^{\mathrm{V}}(\mathbf{\Omega}_{\mathrm{Rx}}, f) \\ F_l^{\mathrm{H}}(\mathbf{\Omega}_{\mathrm{Rx}}, f) \end{bmatrix}^T \begin{bmatrix} \alpha_m^{\mathrm{VV}}(t,f) & \alpha_m^{\mathrm{VH}}(t,f) \\ \alpha_m^{\mathrm{HV}}(t,f) & \alpha_m^{\mathrm{HH}}(t,f) \end{bmatrix} \begin{bmatrix} F_k^{\mathrm{V}}(\mathbf{\Omega}_{\mathrm{Tx}}, f) \\ F_k^{\mathrm{H}}(\mathbf{\Omega}_{\mathrm{Tx}}, f) \end{bmatrix} \cdot \exp\left(-j2\pi v_m t\right) \tag{12}$$

### C. Ray Tracing Simulation

A RT simulation is carried out in an UMa scenario as shown in Fig. 1. The Tx and Rx are placed at a height of $42.5\,\mathrm{m}$ and $1.5\,\mathrm{m}$, respectively. A frequency of $3.7\,\mathrm{GHz}$ is considered and the environment assigned uniform material properties of concrete with a complex permittivity of $2.12 - \mathrm{j}0.48$. Diffracted, diffuse scattered, and transmitted paths are restricted to two orders of interaction while for reflection a maximum order of six is set. The diffuse scattering model used is the Lambertian model with $\mathrm{S} = 0.4$ [8]. It is worthwhile to note that the simulation is carried out using a measurement validated RT tool.

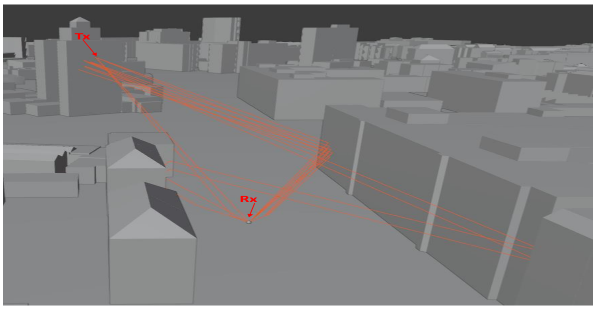


Fig. 1. Illustration of the simulated UMa scenario and a subset of the simulated rays.

### D. Evaluation Criteria

The degree to which the reproduced target CFR matches the target CFR can be evaluated using the frequency response assurance criterion (FRAC) which is commonly used in modal analysis [18], [19]. A FRAC value close to 1 indicates a good match between the target and the realized CFR. The FRAC is defined as:

$$\rho = \frac{|\sum_{p=1}^{P} H_{k,l}^{emu}(t,f)^H H_{k,l}(t,f)|^2}{\sum_{p=1}^{P} H_{k,l}^{emu}(t,f)^H H_{k,l}^{emu}(t,f) \sum_{p=1}^{P} H_{k,l}(t,f)^H H_{k,l}(t,f)}. \quad (13)$$

The error in the magnitude $\boldsymbol{\Delta}\alpha$ can be analyzed by evaluating the equivalent stray signal (ESS) [20], [21] which is commonly used in antenna measurements for comparing the antenna gain pattern when the measurement is performed under slightly different conditions. In contrast to the CFR, a low value of the ESS indicates a good match in the result. The ESS ($\boldsymbol{\Delta}\alpha$) is expressed as:

$$\boldsymbol{\Delta}\alpha(t) = \zeta(t) + 20\log_{10}\left(\frac{1 - 10^{-\beta(t)/20}}{2}\right) \quad (14a)$$

$$\zeta(t) = |\max(\xi_{\text{ref}}(t), \xi_{\text{emu}}(t))| \quad (14b)$$

$$\beta(t) = |\xi_{\text{ref}}(t) - \xi_{\text{emu}}(t)| \quad (14c)$$

$$\xi_{\text{ref}}(t) = 20\log_{10}(|\mathbf{c}_{k,l}(t)|) - \max(20\log_{10}(|\mathbf{c}_{k,l}(t)|)) \quad (14d)$$

$$\xi_{\text{emu}}(t) = 20\log_{10}(|\hat{\mathbf{c}}_{k,l}^{emu}(t)|) - \max(20\log_{10}(|\hat{\mathbf{c}}_{k,l}^{emu}(t)|)) \quad (14e)$$

where $\mathbf{c}_{k,l}(t)$ and $\hat{\mathbf{c}}_{k,l}^{emu}(t)$ are vectors of $P$ frequency bins for the CFR (1) and (12), respectively. On the other hand, the phase error $\boldsymbol{\Delta}\psi$ can be computed as:

$$\boldsymbol{\Delta}\psi(t,f) = |\angle H_{k,l}(t,f) - \angle H_{k,l}^{emu}(t,f)|. \quad (15)$$

## III. Results and Discussion

The FRAC of the UMa scenario considering 1001 channel snapshots is illustrated in Fig. 2. The GLS based approach of delay alignment achieves remarkable performance with a FRAC value of greater than 0.95 for all snapshots for all the three tap configurations. On the other hand, rounding delays to the nearest integer sampling instance has variable performance depending on the MPC structure in the channel. This is undesirable as it impacts negatively on the quality of the VDT.

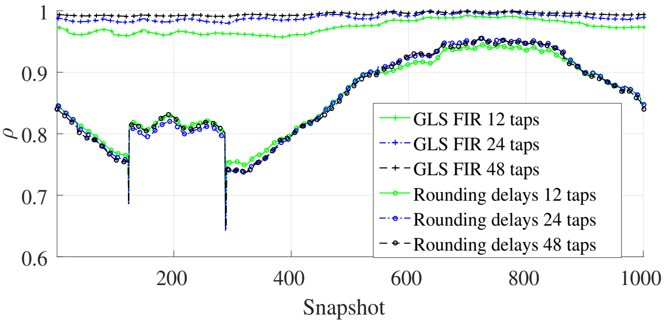


Fig. 2. FRAC for the UMa scenario for the GLS FIR and rounding delays with 12, 24 and 48 taps.

In channel snapshot 288, the rounding delays approach is observed to have the worst performance. As illustrated in the corresponding CIR and CFR in Fig. 3, approximately 20 dB deviation in the CFR occurs for the rounding delays method while the GLS based approach suffers performance deterioration only at frequencies corresponding to the normalized frequency $\omega = \pi$.

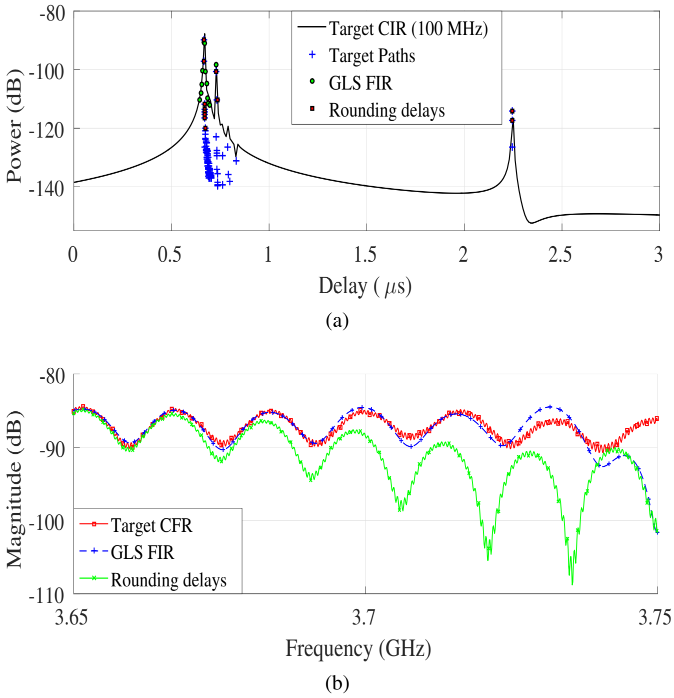


Fig. 3. CIR and CFR of the RT simulated channel with 12 taps at snapshot 288. (a) CIR (b) CFR.

The magnitude and phase errors of each snapshot and for the three tap configurations are illustrated in Fig. 4 while the average magnitude and phase errors are shown in Fig. 5. As observed in the FRAC, the GLS FIR filter based approach results in lower magnitude error in both magnitude

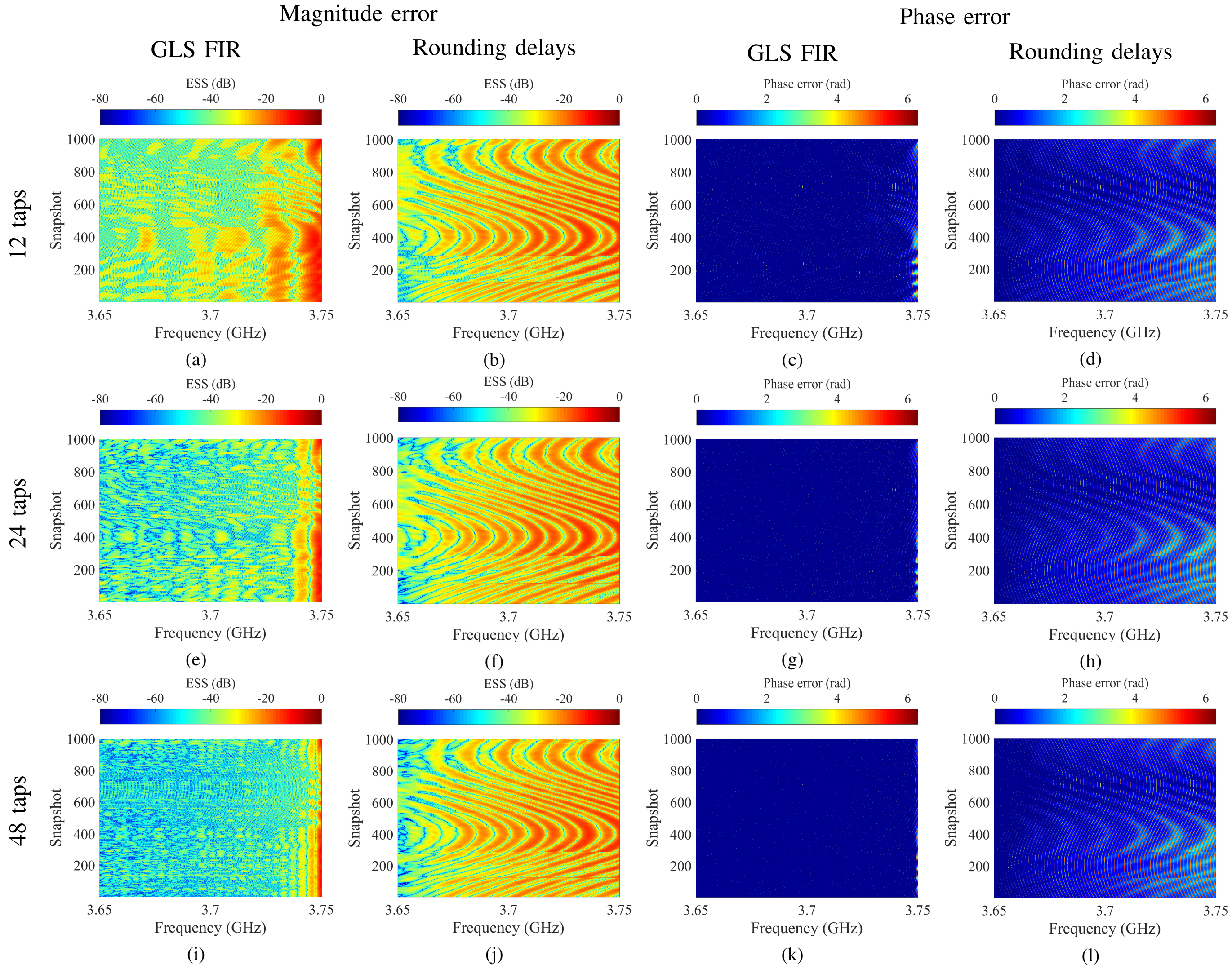


Fig. 4. Magnitude and phase error of the CFR with delay aligned taps for the UMa scenario with 12, 24 and 48 taps.

and phase of the CFR compared to the rounding delays to the nearest integer sampling instance. As the number of taps is progressively increased from 12 to 48, the errors in phase and magnitude for the GLS FIR filter based approach progressively reduce with residual errors only at frequencies corresponding to the normalized frequency $\omega = \pi$. This is because in the tap coefficients are selected from a set of delay aligned coefficients thus a higher number of taps results in a high fidelity reproduction of the CFR. However, this is not necessarily the case with rounding delays method where the additional taps could even result in more severe distortion of the CFR as observed in Fig. 2 for channel snapshots 50 to 390.

## IV. Conclusion

In this paper, delay alignment using band-limited interpolation using the GLS FIR filter was demonstrated to achieve high fidelity reproduction of the CFR compared to rounding delays to the nearest integer sampling instance. This is crucial to ensure that the target CFR is accurately reproduced during VDT. Remarkably, even with 12 taps the GLS FIR filter approach outperforms the rounding delays based approach with 48 taps. Furthermore, the rounding delays method was observed not to guarantee an increase in the match in the CFR with an increase in the number of taps, and in some cases increasing the taps resulted in further performance deterioration. Therefore the GLS FIR based approach is proposed for adjustment of the delay of MPCs of site-specific channels for VDT. In particular in massive MIMO emulation setups, where synchronized emulators can be employed thus availing more taps for each channel during emulation, the GLS FIR based approach promises a high fidelity channel emulation, which would otherwise be inefficiently utilized by the rounding delays approach. One drawback of the GLS FIR filter approach is that the matrix $\mathbf{A}$ in (9) may be ill-conditioned for some channels.

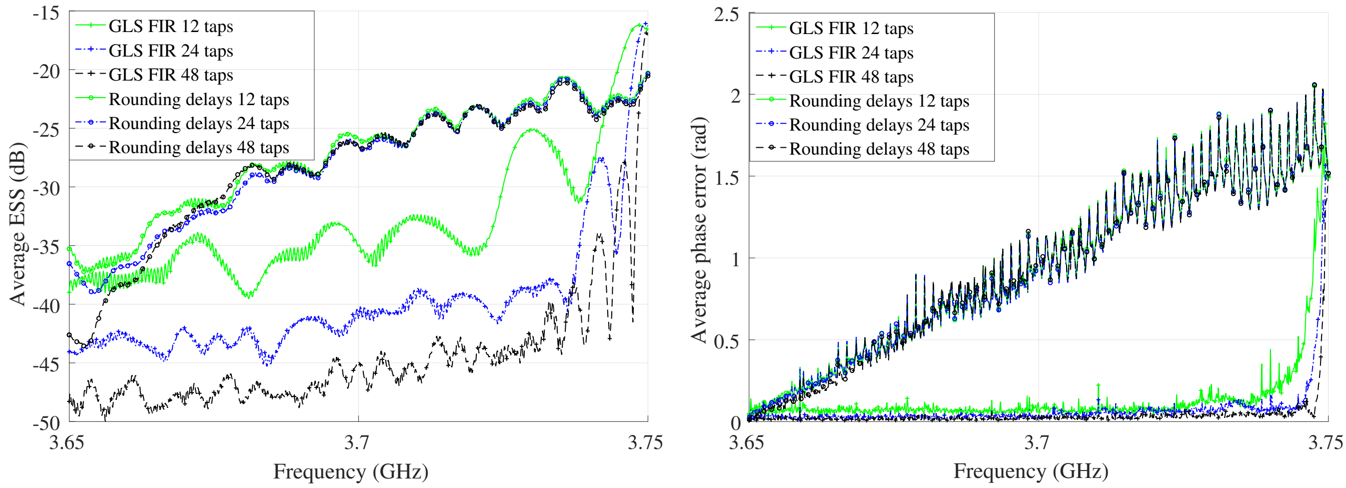


(a) (b)

Fig. 5. Average magnitude and phase error of the CFR with delay aligned taps for the UMa scenario with 12, 24 and 48 taps. (a) Average magnitude error (b) average phase error.


## Acknowledgment

This work was supported by Huawei Technologies.


## References


[1] P. Huang, M. J. Tonnemacher, Y. Du, D. Rajan, and J. Camp, "Towards Massive MIMO Channel Emulation: Channel Accuracy Versus Implementation Resources," *IEEE Trans. Veh. Technol.*, vol. 69, no. 5, pp. 4635–4651, 2020.

[2] W. Fan, I. Carton, P. Kyösti, and G. F. Pedersen, "Emulating Ray-Tracing Channels in Multiprobe Anechoic Chamber Setups for Virtual Drive Testing," *IEEE Trans. Antennas Propag.*, vol. 64, no. 2, pp. 730–739, 2016.

[3] W. Fan, L. Hentilä, F. Zhang, P. Kyösti, and G. F. Pedersen, "Virtual Drive Testing of Adaptive Antenna Systems in Dynamic Propagation Scenarios for Vehicle Communications," *IEEE Access*, vol. 6, pp. 7829–7838, 2018.

[4] J. Cao, D. Kong, M. Charitos, D. Berkovskyy, A. A. Goulianos, T. Mizutani, F. Tila, G. Hilton, A. Doufexi, and A. Nix, "Design and Verification of a Virtual Drive Test Methodology for Vehicular LTE-A Applications," *IEEE Trans. Veh. Technol.*, vol. 67, no. 5, pp. 3791–3799, 2018.

[5] Y. Ji, W. Fan, M. G. Nilsson, L. Hentilä, K. Karlsson, F. Tufvesson, and G. F. Pedersen, "Virtual Drive Testing Over-the-Air for Vehicular Communications," *IEEE Trans. Veh. Technol.*, vol. 69, no. 2, pp. 1203–1213, 2020.

[6] A. W. Mbugua, Y. Chen, L. Raschkowski, L. Thiele, S. Jaeckel, and W. Fan, "Review on Ray Tracing Channel Simulation Accuracy in Sub-6 GHz Outdoor Deployment Scenarios," *IEEE Open J. Antennas Propag.*, vol. 2, pp. 22–37, 2021.

[7] F. Quatresooz, S. Demey, and C. Oestges, "Tracking of Interaction Points for Improved Dynamic Ray Tracing," *IEEE Trans. Veh. Technol.*, vol. 70, no. 7, pp. 6291–6301, 2021.

[8] V. Degli-Esposti, F. Fuschini, E. M. Vitucci, and G. Falciasecca, "Measurement and Modelling of Scattering From Buildings," *IEEE Trans. Antennas Propag.*, vol. 55, no. 1, pp. 143–153, 2007.

[9] J. J. Olmos, A. Gelonch, F. J. Casadevall, and G. Femenias, "Design and Implementation of a Wide-Band Real-Time Mobile Channel Emulator," *IEEE Trans. Veh. Technol.*, vol. 48, no. 3, pp. 746–764, 1999.

[10] Spirent, Spirent Vertex Channel Emulator. [Online]. Available: https://assets.ctfassets.net/wcxs9ap8i19s/1vGUSaaJZCNDi34PeCFgvr/c41cb9ced2f95a00e7c59d643dd6c69c/DS-Spirent-Vertex-Channel-Emulator.pdf

[11] Keysight Technologies, PROPSIM F64, Radio Channel Emulator F8800A, 2021. [Online]. Available: https://www.keysight.com/gb/en/assets/7018-06665/data-sheets/5992-4078.pdf

[12] J. Sozanski and T. Grosch, "Radio Frequency Multipath Channel Emulation System and Method," U.S. Patent US9 130 667B2, Sep 8, 2015.

[13] M. Hofer, Z. Xu, D. Vlastaras, B. Schrenk, D. Löschenbrand, F. Tufvesson, and T. Zemen, "Real-Time Geometry-Based Wireless Channel Emulation," *IEEE Trans. Veh. Technol.*, vol. 68, no. 2, pp. 1631–1645, 2019.

[14] T. Laakso, V. Valimaki, M. Karjalainen, and U. Laine, "Splitting the Unit Delay [FIR/All Pass Filters Design]," *IEEE Signal Process. Mag.*, vol. 13, no. 1, pp. 30–60, 1996.

[15] C. Mehlfuhrer and M. Rupp, "Approximation and Resampling of Tapped Delay Line Channel Models with Guaranteed Channel Properties," in *Proc. IEEE Int. Conf. Acoustics, Speech Signal Process.*, 2008, pp. 2869–2872.

[16] R. Crochiere and L. Rabiner, "Interpolation and Decimation of Digital Signals—A Tutorial Review," *Proc. IEEE*, vol. 69, no. 3, pp. 300–331, 1981.

[17] J. O. Smith, *Spectral Audio Signal Processing*. `http://ccrma.stanford.edu/~jos/sasp/`, Sep 2021, online book, 2011 edition.

[18] W. Heylen and S. Lammens, "FRAC: A Consistent Way of Comparing Frequency Response Functions," in *Proc. Conf. Identification Eng. Syst.*, 1996, pp. 48–57.

[19] R. J. Allemang, "The Modal Assurance Criterion – Twenty Years of Use and Abuse," *Sound and Vibration*, pp. 14–20, 2003.

[20] D. W. Hess, "Historical Background on the Use of Equivalent Stray Signal in Comparison of Antenna Patterns," in *Proc. 5th Eur. Conf. Antennas Propag.*, 2011, pp. 2522–2526.

[21] A. Newell and G. Hindman, "Antenna Pattern Comparison Using Pattern Subtraction and Statistical Analysis," in *Proc. 5th Eur. Conf. Antennas Propag.*, 2011, pp. 2537–2540.